Alzheimer's & Dementia: Diagnosis, Assessment & Disease Monitoring 6 (2017) 122-135

Alzheimer's & Dementia

PART II. State of the Field: Advances in Neuroimaging from the 2016 Alzheimer's Imaging Consortium

Alzheimer's disease: The influence of age on clinical heterogeneity through the human brain connectome

Bradford C. Dickerson[a,b,*], Michael Brickhouse[a,b], Scott McGinnis[a,c], David A. Wolk[d], for the Alzheimer's Disease Neuroimaging Initiative[1]

[a]Department of Neurology, Massachusetts General Hospital, Boston, MA, USA
[b]Department of Neurology, Harvard Medical School, Boston, MA, USA
[c]Department of Neurology, Brigham and Women's Hospital, Boston, MA, USA
[d]Department of Neurology, University of Pennsylvania, Philadelphia, PA, USA

Abstract

Introduction: One major factor that influences the heterogeneity of Alzheimer's disease (AD) is age: younger AD patients more frequently exhibit atypical forms of AD. We propose that this age-related heterogeneity can be understood better by considering age-related differences in atrophy in the context of large-scale brain networks subserving cognitive functions that contribute to memory.
Methods: We examined data from 75 patients with mild AD dementia from Alzheimer's Disease Neuroimaging Initiative. These individuals were chosen because they have cerebrospinal fluid amyloid and p-tau levels in the range suggesting the presence of AD neuropathology, and because they were either younger than age 65 years early-onset AD (EOAD) or age 80 years or older late-onset AD (LOAD).
Results: In the EOAD group, the most prominent atrophy was present in the posterior cingulate cortex, whereas in the LOAD group, atrophy was most prominent in the medial temporal lobe. Structural covariance analysis showed that the magnitude of atrophy in these epicenters is strongly correlated with a distributed atrophy pattern similar to distinct intrinsic connectivity networks in the healthy brain. An examination of memory performance in EOAD dementia versus LOAD dementia demonstrated relatively more prominent impairment in encoding in the EOAD group than in the LOAD group, with similar performance in memory storage in LOAD and EOAD but greater impairment in semantic memory in LOAD than in EOAD.
Discussion: The observations provide novel insights about age as a major factor contributing to the heterogeneity in the topography of AD-related cortical atrophy.

Keywords: Alzheimer's disease; Age; Memory; MRI; Cortical thickness

The cardinal symptoms of Alzheimer's disease (AD) dementia may include impairment of memory, judgment and problem-solving ability, visuospatial abilities, language, praxis, or socioaffective behavior. The clinical diagnosis of AD dementia requires that an individual demonstrates symptoms and signs of decline in at least two of these major cognitive domains [1,2]. Yet, it has been well recognized that within any sample of patients with mild AD dementia, substantial clinical heterogeneity exists [3,4], with one important factor influencing heterogeneity being age [5]. Neuropathologic studies have long-called attention to the fact that it is not amyloid-β plaques that drive this heterogeneity, but rather the localization and severity of neurofibrillary tangles and associated neuronal and glial

[1]Data used in preparation of this article were obtained from the Alzheimer's Disease Neuroimaging Initiative (ADNI) database (adni.loni.usc.edu). As such, the investigators within the ADNI contributed to the design and implementation of ADNI and/or provided data but did not participate in analysis or writing of this report. A complete listing of ADNI investigators can be found at http://adni.loni.usc.edu/wp-content/uploads/how_to_apply/ADNI_Acknowledgement_List.pdf.

*Corresponding author. Tel.: 6177265571; Fax: 6177265760.
E-mail address: brad.dickerson@mgh.harvard.edu

http://dx.doi.org/10.1016/j.dadm.2016.12.007

degeneration that predict the particular clinical syndrome exhibited by a patient [6–8]. A recently developed system for classifying the heterogeneity of neuropathology in AD subdivides cases based on neurofibrillary pathology into "typical," "limbic predominant," or "hippocampal sparing" subtypes [9]. One major factor that seems to influence the topography of neurodegeneration in AD is age, with younger patients being more likely to exhibit neurodegeneration that is more prominent in isocortical temporoparietal regions ("hippocampal sparing") and older patients showing more prominent neurodegeneration in the hippocampus and other medial temporal lobe (MTL) structures ("limbic predominant") [10–14].

In considering the relationship of clinical heterogeneity to varying topographical patterns of neurodegeneration, it is important to examine AD-related neurodegeneration within the context of large-scale brain networks in the human brain [15]. Resting-state functional magnetic resonance imaging (fMRI) studies have shown that intrinsic connectivity networks (ICNs) correspond very well to known anatomic connectivity from tract-tracing studies in nonhuman primates [16] and to the topography of functional networks that are activated during the performance of specific cognitive tasks in fMRI experiments [17]. The anatomic organization of ICNs provides an organizing framework for testing hypotheses about AD-related atrophy.

These and related methods have been used to demonstrate that imaging measures of the localization of neurodegenerative pathology in AD overlap substantially with a large-scale network commonly referred to as the default mode network (DMN) [18–23], which plays important roles in episodic memory among other abilities [24]. This has led to the hypothesis that, early in its course, AD preferentially targets the DMN [18,21]. Although the importance of the DMN in AD is indisputable, the emphasis on this network is somewhat surprising given the abnormalities in multiple cognitive domains are present at the time of a clinical diagnosis of AD dementia [2] and even in prodromal AD (multidomain mild cognitive impairment [MCI]) [25].

A number of questions remain outstanding regarding the degree to which AD is a single versus multiple network disease and the influence of age on network neurodegeneration in AD. Here we sought to address these questions by examining the relationships between the localization of large-scale ICNs derived from functional connectivity fMRI studies of healthy young adults and the localization and magnitude of atrophy in mild AD dementia with early-onset versus late-onset AD. Our objective in the present study was to test three hypotheses in patients with mild dementia due to AD: Older patients will demonstrate more prominent atrophy in anterior MTL (aMTL) regions, whereas younger patients will demonstrate more prominent atrophy in posterior temporoparietal regions. Within the entire patient group, the relative magnitude of atrophy within the aMTL "epicenter" will correlate with atrophy in areas of the rostroventral DMN or anterior temporal/paralimbic network, whereas the relative magnitude of atrophy within atrophy within the posterior temporoparietal epicenter will correlate with atrophy in the caudal-dorsal default mode network. In addition, we propose that the clinical heterogeneity of AD can be better understood by examining large-scale brain networks at a finer scale, where the DMN fractionates into multiple distinct networks. Finally, we predict that the magnitude of atrophy of key regions within these networks will predict the types and severity of impairment in specific memory processes.

1. Methods

1.1. Participants

Data used in the preparation of this article were obtained from the Alzheimer's Disease Neuroimaging Initiative (ADNI) database (adni.loni.usc.edu). The ADNI was launched in 2003 as a public-private partnership, led by a principal investigator Michael W. Weiner, MD. The primary goal of ADNI has been to test whether serial MRI, positron emission tomography (PET), other biological markers, and clinical and neuropsychological assessment can be combined to measure the progression of MCI and early AD. For up-to-date information, see www.adni-info.org.

For the current analysis, we selected individuals with a diagnosis of AD dementia with cerebrospinal fluid amyloid-$\beta \leq 192$ pg/mL and phospho-tau > 23 pg/mL, supportive of the likely presence of amyloid plaques and neurofibrillary tangles [26]. Furthermore, we focused on individuals whose age was consistent with early-onset AD (age < 65 years) and those whose age was consistent with late-onset AD (age > 80 years). Detailed diagnostic, inclusion, and exclusion criteria are described on the ADNI web site (http://www.adni-info.org/).

For the control groups, we selected individuals with a diagnosis of cognitively normal with cerebrospinal fluid amyloid-$\beta > 192$ pg/mL, supportive of the likely absence of amyloid plaques [26]. Because there were relatively few such individuals younger than 65, we selected individuals ≤ 70, providing a young control group of 69 individuals with a mean age of 66.8 (standard deviation [SD] 2.5, range 56–70), education 16.7 years (SD 2.6), 57% females, a single apolipoprotein E (*APOE*) ε4 carrier. Similarly, for the older control group, we selected individuals $\geq$age 77 years, providing a young control group of 41 individuals with a mean age of 80.1 (SD 2.8, range 77–85), education 17.5 years (SD 2.5), 54% females, 5 *APOE* ε4 carriers.

1.2. Standard protocol approvals, registrations, and patient consents

Each participant gave written informed consent in accordance with institutional Human Subjects Research Committee guidelines.

1.3. MRI imaging and analysis

MRI scans were collected on a 1.5-T or 3.0-T scanner using a standardized MPRAGE protocol: sagittal plane, TR/TE/

TI, 2400/3/1000 ms, flip angle 8°, 24-cm FOV, 192 × 192 in-plane matrix, 1.2-mm slice thickness [27]. Fully preprocessed scans were downloaded for analysis. 71% of controls and 72% were scanned on a 1.5T scanner.

T1 image volumes were examined quantitatively by a cortical surface-based reconstruction and analysis of cortical thickness, using a combination of hypothesis-driven and exploratory analysis approaches as described in multiple previous publications [28–34].

1.4. Neuropsychological measures

We examined baseline memory testing from the ADNI database. Although our central analysis was focused on the Rey Auditory Verbal Learning Test (AVLT) [35], we also examined brain-behavior relationships with a proxy measure of semantic memory, the Boston Naming Test supported with both semantic and phonemic cueing. Briefly, the AVLT consists of five learning trials in which a list of 15 words is read and the subject is asked to immediately recall as many items as possible. For the present analysis, we included trial-1 encoding and total learning (the sum of items encoded over all five trials). After an interference list of 15 novel words is read and recalled, subjects are then asked to recall words from the initial list (5-minute delayed recall). A 30-minute delayed recall trial and recognition test follow. We focused here on 30-minute delayed retention (the number of items recalled divided by the number of items encoded on the last learning trial). For the recognition test, subjects are presented with a list of the 15 studied words and 15 nonstudied foils and are asked to circle all words previously studied. To account for false alarms to nonstudied items, we calculated a measure of discriminability, d-prime (d′), which was calculated in a standard fashion based on classic signal detection theory [36]. Additionally, because d′ is undefined when either proportion is 0 or 1, we used standard formulas to convert these values: Hits = (#Hits + 0.5)/(#studied items + 1) and FA = (#FA + 0.5)/(#unstudied items + 1). Thus, for verbal episodic memory, we used AVLT trial-1 encoding, total encoding, delayed retention, and recognition discriminability.

In the ADNI version of the Boston Naming Test [37], subjects are asked to name 30 black and white line drawings, each of a single object. The subject is given up to 20 seconds to respond, and if the initial response is determined to be an error based on visuoperceptual misinterpretation, a semantic cue is offered. A phonemic cue is offered for all incorrect or nonresponses, regardless of whether there was a visuoperceptual error. The test is discontinued if there are six consecutive failures, inclusive of responses to semantic cueing. The total score (our semantic memory measure) is the sum of the initial correct responses plus additional correct responses after a semantic prompt (if given). Thus, a failure after both phonemic and semantic cueing is likely indicative of a semantic memory deficit.

For each of these tests, we calculated a Z score for each AD patient's performance compared to the distribution of performance in age-matched control group. That is, for EOAD patients, we calculated Z scores using the younger amyloid-negative cognitively normal control group, and for LOAD patients, we used the older control group.

1.5. Statistical analysis

Cortical thickness measures were mapped to the inflated surface of each participant's reconstructed brain (Fischl, Sereno and Dale 1999), which were then mapped to the standard FreeSurfer average template (fsaverage). This procedure allows visualization of data across the entire cortical surface (i.e., both the gyri and sulci) without interference from cortical folding. The data were smoothed on the surface using an iterative nearest-neighbor averaging procedure. One hundred iterations were applied, which is equivalent to applying a two-dimensional Gaussian smoothing kernel along the cortical surface with a full-width/half-maximum of 18.4 mm. Data were then resampled for participants into a common spherical coordinate system (Fischl, Sereno, and others 1999). The procedure provides accurate matching of morphologically homologous cortical locations among participants on the basis of each individual's anatomy, while minimizing geometric distortion, resulting in a mean measure of cortical thickness for each group at each point on the reconstructed surface.

For the primary analyses, statistical surface maps were generated by computing a two-class general linear model for the effect of membership in (1) each of the AD groups when compared to each of the age-matched control groups. For these exploratory analyses, a statistical threshold of $P < .01$ was used. Structural covariance analysis was performed by using a one-class general linear model, including all AD patients, and using the cortical thickness from within each of the regions of interest as the independent variable with cortical thickness across the remainder of the cortical mantle as the dependent variable.

In addition, tests of group differences were performed using chi-square analysis (for frequencies) or analysis of variance (for continuous measures) with post hoc pairwise comparisons where relevant; a = 0.05. Because effect sizes were expected to be subtle and strong a priori hypotheses were being tested, no multiple comparisons correction procedures were performed. Statistical analyses were performed using IBM SPSS 21.0.

2. Results

2.1. Demographic and clinical characteristics of samples

Table 1 shows the demographic and clinical characteristics of the sample. The LOAD group ($n = 49$) had a slightly higher percentage of females and a slightly lower rate of *APOE* ε4 carriers than the EOAD group ($n = 26$). Otherwise, the groups were well matched.

2.2. Spatial topography of atrophy in EOAD versus LOAD

We confirmed the clear difference in the spatial topography of atrophy in EOAD versus LOAD. In EOAD,

Table 1
Clinical and demographic characteristics of participants

Variable	EOAD	LOAD
Age	60.5 (2.8)	84.3 (3.1)****
Gender (% female)	50% female	67% female
Education	16 (1.9)	15.2 (3.3)
MMSE	22.7 (2.1)	22.5 (2.1)
CDR sum-of-boxes	4.9 (1.5)	4.9 (1.8)
APOE ε4 (% carriers)	72%	61%*
AVLT trial-1 encoding	−1.7 (0.95)	−1.1 (0.86)***
AVLT total encoding	−3.1 (0.77)	−2.1 (0.78)****
AVLT delayed retention	−1.8 (1.2)	−2.0 (0.99)
AVLT recognition discriminability	−2.4 (1.2)	−2.6 (1.0)
BNT cued naming (semantic memory)	−1.3 (2.3)	−5.7 (4.5)****

Abbreviations: MMSE, Mini–Mental State Examination; CDR, clinical dementia rating; *APOE*, apolipoprotein E; EOAD, early-onset Alzheimer's disease; LOAD, late-onset Alzheimer's disease; AVLT, Auditory Verbal Learning Test; BNT, Boston Naming Test.

*$P < .05$; ***$P < .005$; ****$P < .001$.

atrophy is most prominent in the posterior cingulate cortex (PCC) and precuneus, inferior parietal lobule, and caudal ventral and lateral temporal cortex, with a small degree of dorsolateral prefrontal cortical (DLPFC) involvement. The aMTL and temporal pole were relatively spared. In LOAD, the aMTL and anterior temporal cortex were prominently atrophied, with additional prominent effects in caudal ventral and lateral temporal cortex, PCC, inferior parietal, and DLPFC. See Fig. 1 for cortical surface maps of these effects.

When the statistical threshold was made more stringent so as to identify a single "epicenter" of most prominent atrophy in each of these age-related subtypes of AD, we identified the PCC/precuneus as the epicenter in EOAD and the aMTL cortex as the epicenter in LOAD. The localization of the aMTL epicenter in LOAD overlaps with both entorhinal and perirhinal cortices, based on topographic mapping of an independent sample of postmortem brains that had been examined cytoarchitectonically [38,39]. Comparison of the map in Fig. 2A with that of Fig. 1A might suggest that—rather than the precuneus—the left inferior parietal cortex should be the epicenter because it demonstrates a slightly larger difference in thickness (Fig. 1A). Yet the inferior parietal cortex also exhibits larger variance, so when the map of statistical significance is thresholded stringently (Fig. 2A), the precuneus demonstrates the most statistically significant effect. Interestingly, as can be seen in Fig. 3B, these two regions show strong structural covariance, and the network maps shown in Fig. 4 demonstrate that they are clearly both nodes of the dorsal default mode network.

An examination of the thickness of these epicenters in EOAD and LOAD versus the two control groups matched in age to the patient groups (Fig. 5) further illustrates the

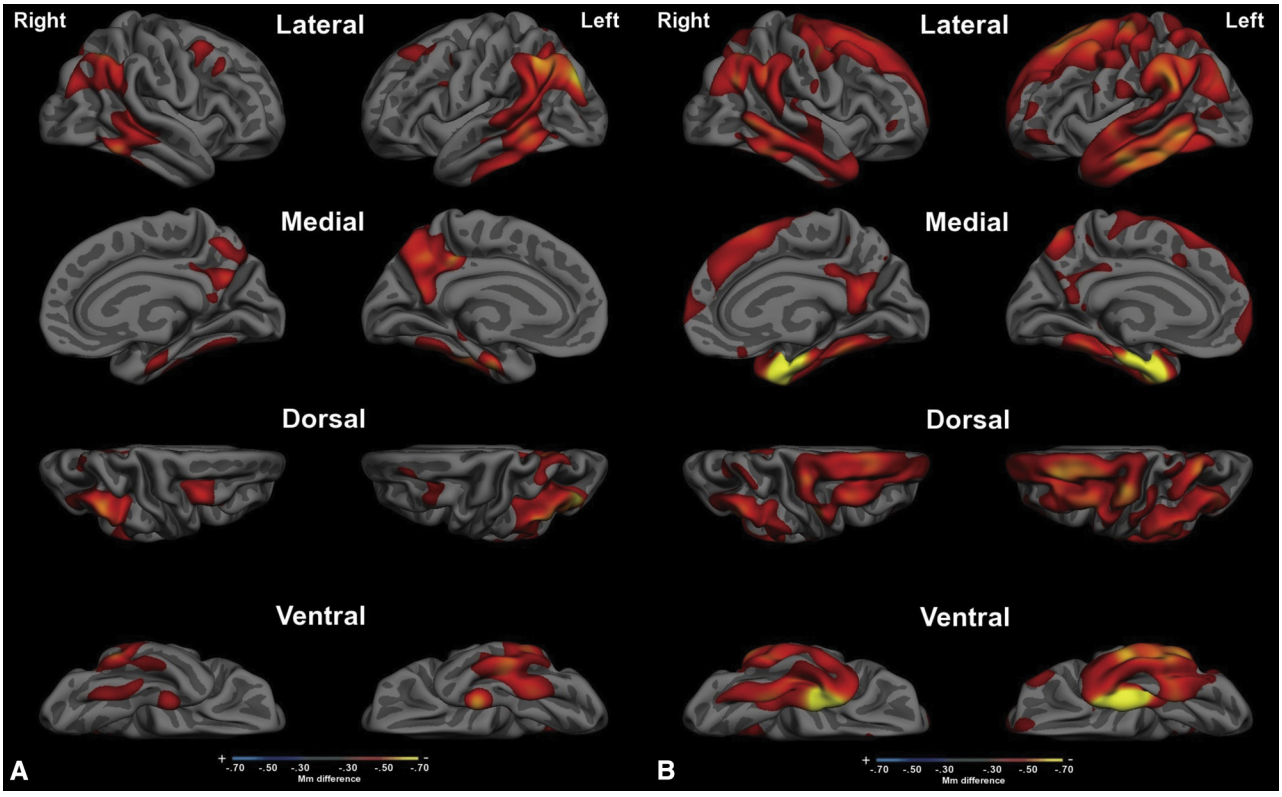

Fig. 1. Cortical atrophy maps of (A) early-onset Alzheimer's disease versus age-matched controls and (B) late-onset Alzheimer's disease versus age-matched controls. Maps depict regions in which the thickness of the cortex in AD patients is at least 0.3 mm thinner than controls, and all are statistically significant ($P < .01$). Maps are shown on a partially inflated average cortical surface template from 40 individuals (fsaverage). Abbreviation: AD, Alzheimer's disease.

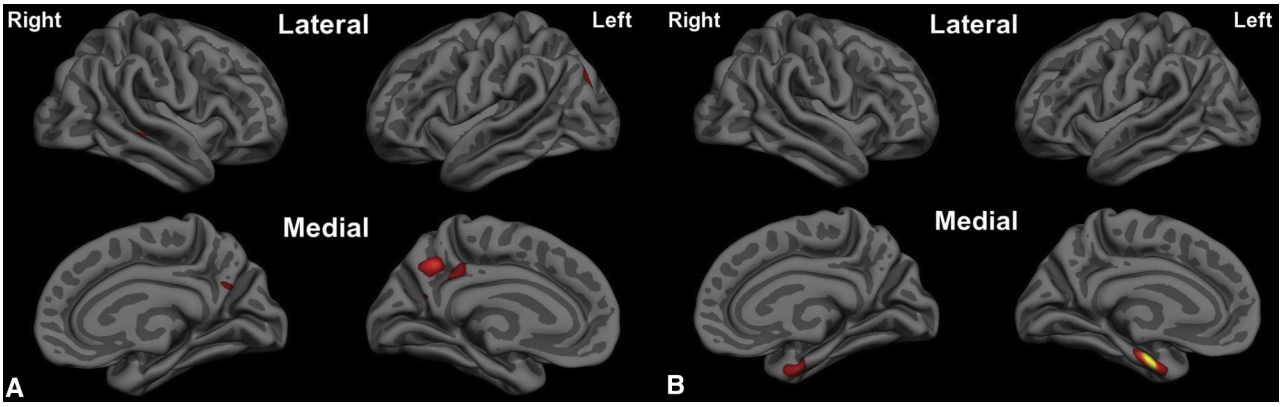

Fig. 2. Epicenters of cortical atrophy. (A) The posterior cingulate cortex/ventral precuneus is the epicenter of cortical atrophy in early-onset Alzheimer's disease versus age-matched controls ($P < 1 \times 10^{-7}$). (B) The anterior medial temporal (entorhinal and perirhinal) cortex is the epicenter of cortical atrophy in late-onset Alzheimer's disease versus age-matched controls ($P < 1 \times 10^{-11}$).

age-dependent dissociation between these cortical regions with regard to the effects of AD.

2.3. Structural covariance mapping of these epicenters

A structural covariance analysis of the entire sample of EOAD + LOAD patients revealed distinct patterns for the PCC EOAD epicenter versus the aMTL LOAD epicenter (Fig. 3). Structural covariance mapping of the PCC revealed bilateral PCC, the inferior parietal lobule, posterior lateral temporal cortex, and lateral and medial superior frontal gyrus. Structural covariance mapping of the aMTL revealed a distinct pattern of bilateral aMTL cortex (including entorhinal and perirhinal cortex), temporal pole, and anterior lateral and ventral temporal cortex, as well as subgenual cingulate cortex. A limitation of these covariance maps is that they were generated within the same sample from which the epicenters were defined; future analyses will aim to determine whether similar covariance is found in independent samples, including controls.

An examination of the overlap of these two maps demonstrated three major findings. First, there is minimal overlap between them except in caudal lateral temporal regions (Fig. 3). Second, the union of these two maps shows a topography of atrophy that is very similar to the original AD signature [40] (Fig. 6). The original AD signature included patients with a relatively wide age range, although most

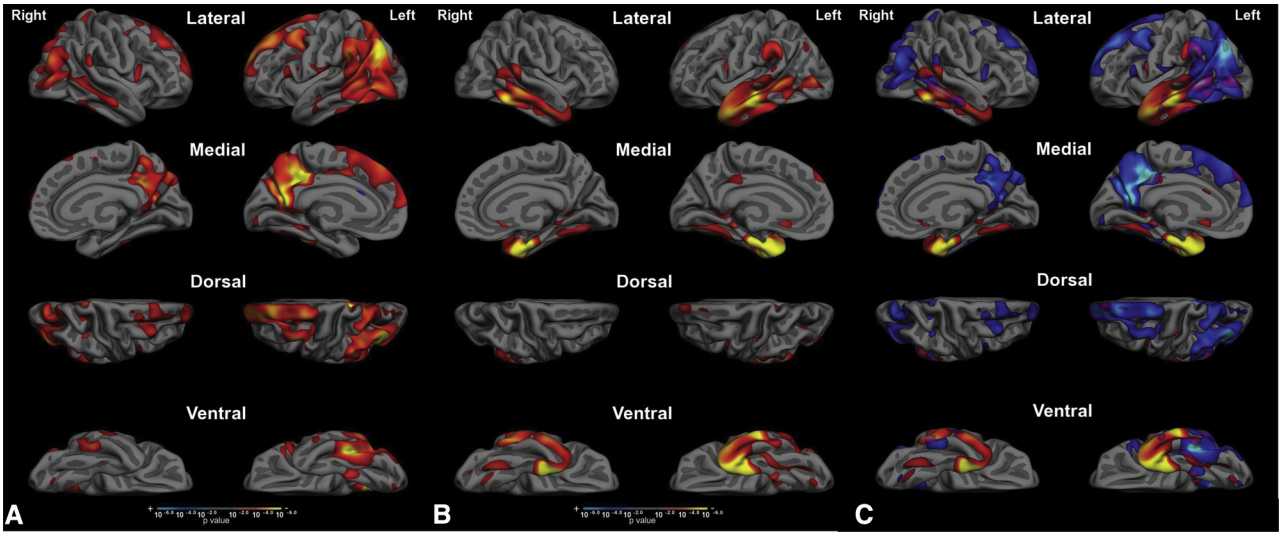

Fig. 3. Structural covariance analyses of each of the two epicenters reveal two largely distinct distributed patterns of atrophy. (A) Regions where cortical atrophy is correlated with PCC atrophy include bilateral PCC, the inferior parietal lobule, posterior lateral temporal cortex, and lateral and medial superior frontal gyrus. (B) Regions where cortical atrophy is correlated with aMTL atrophy include entorhinal and perirhinal cortex, temporal pole, and anterior lateral and ventral temporal cortex, as well as subgenual cingulate cortex. (C) An overlap map comparing the EOAD-epicenter structural covariance map to the LOAD-epicenter structural covariance map clarifies these as two nearly independent maps, with minimal overlap primarily in the caudal lateral temporal cortex, with smaller regions of overlap in the angular gyrus and posterior cingulate and retrosplenial cortex. Abbreviation: PCC, posterior cingulate cortex.

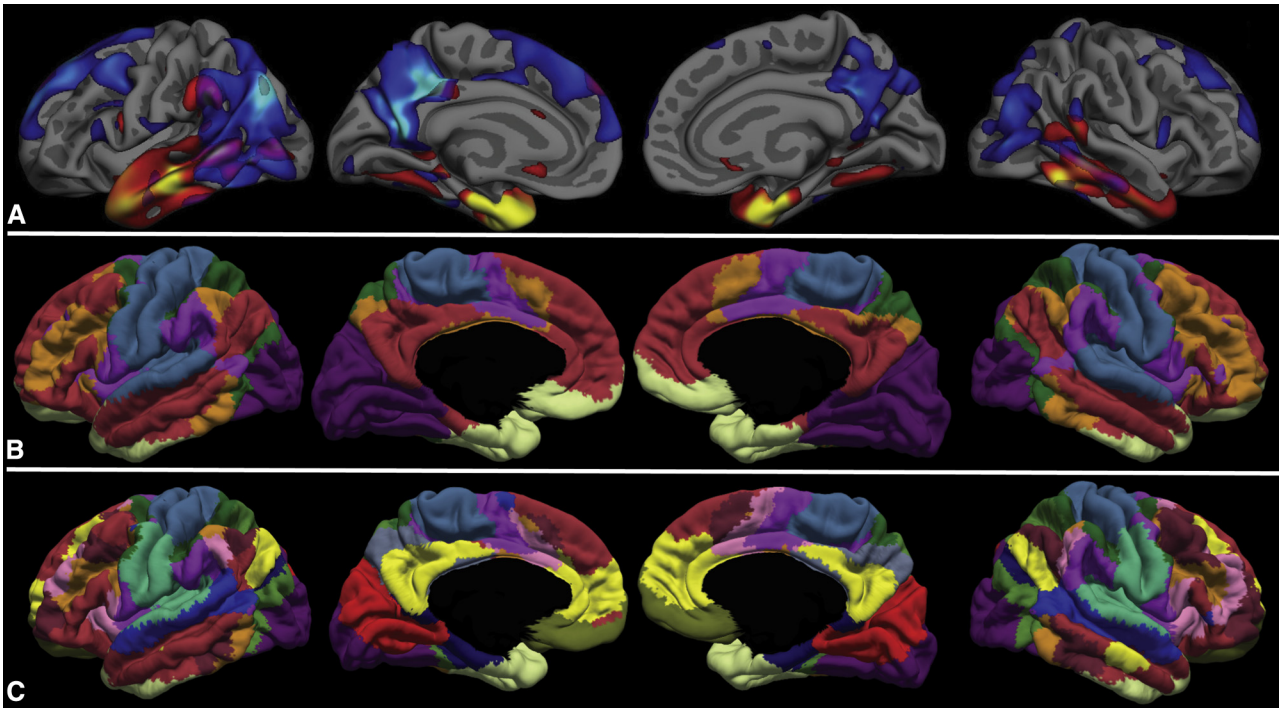

Fig. 4. The overlap of this spatial pattern of atrophy and the localization of large-scale brain networks clearly demonstrate the involvement of multiple networks at the mild clinical stage of AD dementia, with a pattern that differs based on age of onset. Compared with the seven-network parcellation by Yeo et al. (2011) (B), the EOAD-epicenter structural covariance map (A) largely overlaps with DMN and frontoparietal executive control networks, whereas the LOAD-epicenter structural covariance map largely overlaps with the anterior temporal/paralimbic network. Compared with the Yeo et al. (2011) 17-network parcellation (C), the EOAD-epicenter structural covariance map overlaps with dorsal DMN and language networks, whereas the LOAD-epicenter structural covariance map overlaps with the anterior temporal/paralimbic network. Thus, the overlap of AD-related atrophy and large-scale brain networks depends both on the characteristics of AD patients (with age being one major factor) and the scale at which brain networks are examined. Abbreviations: AD, Alzheimer's disease; DMN, default mode network.

were late onset. Major regions include aMTL and ventral temporal cortex, temporal pole, lateral temporal cortex, inferior parietal lobule, PCC and precuneus, and medial and lateral superior frontal gyrus.

Third, the overlap of this spatial pattern of atrophy and the localization of large-scale brain networks clearly demonstrate the involvement of multiple networks at the mild clinical stage of AD dementia, with a pattern that differs based on age of onset. Compared with the seven-network parcellation by Yeo et al. (2011) (Fig. 4A), the localization of atrophy in EOAD is largely confined to DMN and frontoparietal executive control network,

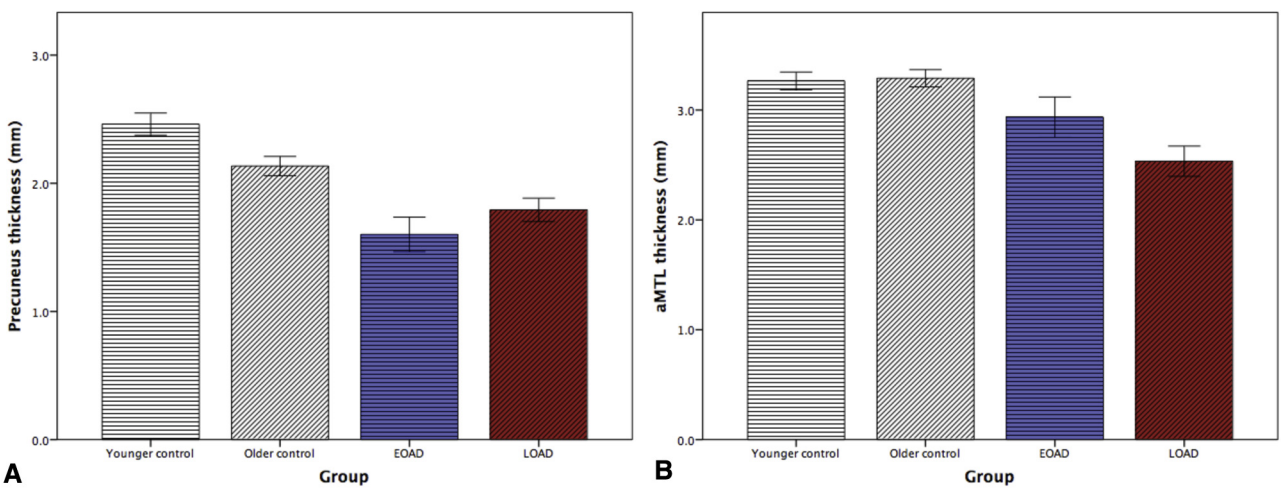

Fig. 5. Comparison of cortical thickness of epicenters of cortical atrophy. Bar graphs depict thickness of (A) precuneus which is the epicenter of EOAD and (B) anterior medial temporal cortex which is the epicenter of LOAD, compared to age-matched younger and older control groups of cognitively normal, amyloid-negative individuals. Abbreviation: aMTL, anterior medial temporal lobe.

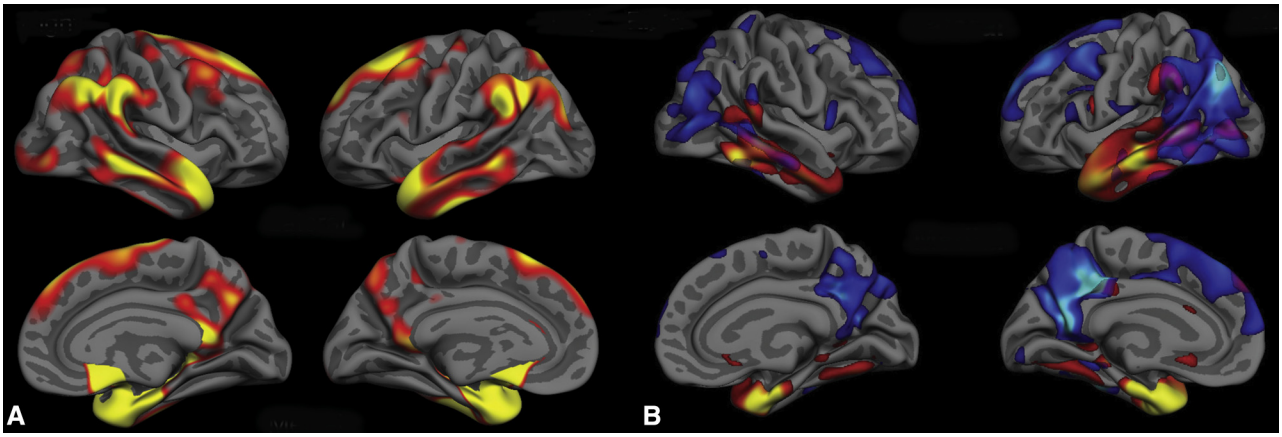

Fig. 6. The EOAD-epicenter and LOAD-epicenter structural covariance overlap map (B) shows a topography that is very similar to the original AD signature (A), which compared patients with mild AD dementia ($n = 73$) to age-matched controls ($n = 194$). The original AD signature included patients with a relatively wide age range, although most were late onset. Major regions include anterior MTL and ventral temporal cortex, temporal pole, lateral temporal cortex, inferior parietal lobule, PCC and precuneus, and medial and lateral superior frontal gyrus. Abbreviations: AD, Alzheimer's disease; MTL, medial temporal lobe; PCC, posterior cingulate cortex.

whereas in LOAD, the localization of atrophy is primarily evident in the anterior temporal/paralimbic network. Compared with the 17-network parcellation by Yeo et al. (2011) (Fig. 4B), atrophy in EOAD can be seen in dorsal DMN and language networks, whereas in LOAD, it is present in the anterior temporal/paralimbic network. Thus, the overlap of AD-related atrophy and large-scale brain networks depends both on the characteristics of AD patients (with age being one major factor) and the scale at which brain networks are examined.

2.4. *Localization of atrophy in relation to memory systems*

Finally, the relationship of atrophy in EOAD versus LOAD to memory performance measures demonstrates that age influences how AD disrupts dissociable memory processes through its effects on key nodes of distinct memory systems. On the AVLT, trial-1 memory encoding is relatively more impaired in EOAD ($Z = -1.7$) than in LOAD ($Z = -1.1$). On total learning across all five trials, these effects are much more pronounced, with EOAD showing a relatively little learning with repeated encoding ($Z = -3.1$) while LOAD showed prominent but lesser impairment ($Z = -2.1$). In contrast, the EOAD group showed similar impairment on delayed retention ($Z = -1.8$) compared to the LOAD group ($Z = -2.0$). Recognition discriminability was also similar in the EOAD group ($Z = -2.4$) than in the LOAD group ($Z = -2.6$). Fig. 7 illustrates these findings. Repeated-measures ANOVA demonstrates that the groups show significant differences in the two encoding measures as well as the semantic memory measure (Table 1).

3. Discussion

In the debates about whether AD is primarily a disease of the DMN or also involves other networks, age has received relatively little attention. Here we reinforce previous observations [10,11,13,14,41–48] that older people with mild AD dementia have more prominent atrophy in aMTL regions, whereas younger people with mild AD dementia have more prominent atrophy in posterior temporoparietal regions, especially the PCC. Structural covariance analyses demonstrate that patients with greater atrophy in the aMTL "LOAD epicenter" also exhibit a larger degree of atrophy in areas of the anterior temporal/paralimbic

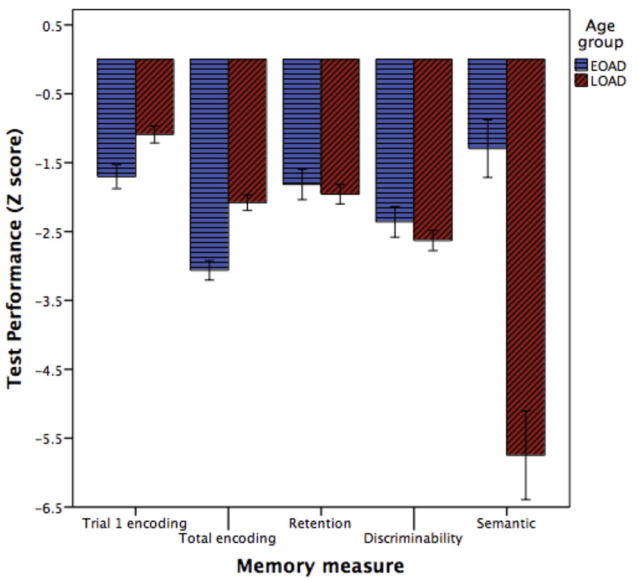

Fig. 7. Patients with EOAD are more impaired than those with LOAD on Rey Auditory Verbal Learning Test trial-1 encoding and total learning across all trials. The groups are similarly impaired on delayed retention and recognition discriminability, although the LOAD may be very slightly more impaired on these measures. In contrast, patients with LOAD are more impaired than those with EOAD on semantic memory measured using the Boston Naming Test.

network (which includes but extends more rostrally to the usual anterior-ventral MTL subsystem of the DMN [49]). In contrast, those with greater atrophy in the PCC "EOAD epicenter" exhibit a larger degree of atrophy in a distinct set of brain regions mostly, but not exclusively, including dorsal regions of the DMN (the frontoparietal DMN subsystem [49]). Finally, the clinical heterogeneity of memory impairments in AD fit with these anatomical observations, with encoding-related measures—which are supported in part by isocortical lateral temporal, parietal, and frontal and medial parietal cortices—showing more prominent impairment in EOAD and semantic memory—supported largely by temporal pole and anterior temporal cortex—showing more prominent impairment in LOAD. Memory storage was similarly impaired in both groups. To contextualize these new findings, we will first review traditional anatomical models of MTL memory systems [50,51], which provide a foundation for understanding how these two subsystems support memory functions.

3.1. Traditional anatomical models of the MTL memory systems

Multiple isocortical areas are important for episodic memory, including prefrontal and parietotemporal association areas that mediate perceptual aspects of encoding [52], working memory, effortful encoding and retrieval, source monitoring, and other functions that are essential to conscious recollection [53–55]. Animal studies have shown that reciprocal projections from isocortical association areas strongly converge onto the MTL, which are funneled into the hippocampus via the parahippocampal, perirhinal, and the entorhinal cortices [56,57]. The perirhinal cortex receives inputs from areas concerned with identifying the identity of objects (the "what" pathway), whereas the parahippocampal cortex receives inputs from many areas involved in processing the spatial content of sensory information (the "where" pathway). The pattern in which the fibers from both pathways—via medial and lateral entorhinal cortex, respectively—terminate in hippocampal targets differs between those arriving in CA3 and dentate gyrus and those in CA1 and subiculum, such that information passing through the entorhinal cortex is combined on the same neurons in the dentate gyrus and CA3 but arrives in separate neuronal populations in the subiculum and CA1, a topographical pattern that may support the ability of the hippocampus to both associate and distinguish events and the context in which they appear [58]. The localization of efferent and afferent connectivity also varies along the long axis of the hippocampus and MTL cortex, providing the basis for two major dissociable MTL-cortical networks [59,60]. This anatomical framework illustrates the segregation and integration of basic functional-anatomic mechanisms that support episodic memory processes, which are beginning to be illuminated further in humans via neuroimaging. For example, resting-state functional MRI has been used to demonstrate the distinction between subnetworks within the MTL memory system, including the rostral hippocampal-perirhinal network versus the caudal hippocampal-parahippocampal-retrosplenial network [49,61,62]. As reported here, age appears to be an important modulator of the integrity of these MTL networks in the context of mild AD.

3.2. Rostral hippocampal-perirhinal subsystem

Anterior MTL regions—including entorhinal and perirhinal cortices and anterior hippocampus—are heavily interconnected with the ventral and lateral anterior temporal cortex as well as the temporal pole. The entorhinal and perirhinal cortices share strong reciprocal connections with the orbital and medial prefrontal cortex, as well as the amygdala [63–66]. Along with lateral orbitofrontal cortex, the lateral amygdala is critical for integrative sensory processing, and these structures are probably involved with assigning value or relevance to highly processed visual information in anterior temporal cortical regions; the medial amygdala shares connectivity with reward-related structures including the nucleus accumbens (to which the temporal pole also connects). Taken together, these anatomic studies, as well as functional neuroimaging investigations and studies of patients with semantic dementia as well as AD, suggest a key role for the temporal pole and other anterior temporal structures in the integration of multimodal sensory and conceptual information with episodic memory to guide valuation and approach- or avoidance-related behavior [67,68]. Ultimately, this subsystem works together to process the identity of objects in the dual dimensions of encyclopedic knowledge (semantic memory and conceptual processing) and personal valuation, both linked to past personal episodic experience [62]. Yet, although this anterior temporal subsystem is primarily thought to be a multimodal integration convergence zone focused on object identity and association [69], it also shares connectivity to the dorsal DMN [70], particularly through the retrosplenial cortex [71,72], inferior parietal lobule [57,73], and ventromedial prefrontal cortex, which is thought to bring in a variety of elements of context.

The aMTL has long been considered the origin of neurodegeneration of AD [74,75], and the area of most prominent atrophy [40,76], including in preclinical and prodromal phases [30,77]. Despite the fact that aMTL atrophy is a widely replicated sensitive biomarker of early AD-related neurodegeneration [78], this region is often spared in EOAD, whether measured via MRI *in vivo* [47] or by postmortem autopsy examination [9]. In patients with dementia associated with amyloid-β neuritic plaques and hyperphosphorylated neurofibrillary tangles, the mechanisms that influence whether MTL regions are relatively spared remain poorly understood. The presence of an *APOE* ε4 allele is one well-documented factor that is associated with more prominent MTL neurodegeneration [33]. Although *APOE* ε4 is well known to facilitate amyloid-β production and deposition, it also reduces the effectiveness of neuronal repair mechanisms in the setting of

toxicity [79]. In addition, the ε4 allele promotes tau phosphorylation and neurofibrillary tangle production [80]. We believe that age and *APOE* ε4 exert similar effects on MTL neurodegeneration. Age is associated with a primary MTL tauopathy [81] such that older adults have pre-existing MTL pathology independent of plaque and tangle AD pathology, which then may accelerate this process. In contrast, younger adults do not have as much MTL tauopathy and, thus, tend to display relatively greater involvement of isocortical networks although these are also involved in older adults. Similarly, those carrying the *APOE* ε4 allele would also be expected to have more prominent aMTL neurodegeneration that *APOE* ε4 noncarriers when matched for age. Thus, an older AD patient who is an *APOE* ε4 carrier would be predicted through this "dual hit" model to display the highest levels of MTL neurodegeneration while a young-onset *APOE* ε4 noncarrier would have the least MTL neurodegeneration. Given the effect of *APOE* ε4 on disease onset, however, this full effect may be infrequent in LOAD cohorts such as described here. Regardless, the potential mechanisms through which age and *APOE* ε4 exert their effects will be illuminated by comparing amyloid and tau PET or cerebrospinal fluid measures to atrophy.

3.3. Caudal hippocampal-parahippocampal-retrosplenial subsystem

The caudal MTL—including caudal hippocampus and posterior parahippocampal cortex—shares stronger connectivity than the aMTL with retrosplenial cortex, posterior cingulate cortex, precuneus, angular gyrus, and medial prefrontal cortex [61,82]. The caudal MTL is known to have robust reciprocal connections with retrosplenial cortex [71,72] and posterior cingulate cortex [83]. Weaker reciprocal connections are present between caudal MTL and the precuneus [83,84] and inferior parietal lobule [57,73], as well as medial prefrontal cortex [66,85]. These observations from macaque tract-tracing studies have been supported by human functional connectivity MRI investigations [61,82,86], which indicate that the caudal MTL is primarily affiliated with major DMN hubs while the aMTL subsystem is weakly linked to these regions and best considered a distinct subsystem [24,49]. This system is engaged during episodic memory retrieval [87], especially including autobiographical memory [88]. Studies of prospective memory—the use of past experience to simulate future events—have also emphasized the engagement of this subsystem [89–91]. Ultimately, this subsystem is thought to process a variety of aspects of the contextual properties of stored episodes, including spatial location [92], object contextual association [93], and temporal sequence [94].

The caudal MTL is also well established as undergoing neurodegeneration in AD, although in typical cases to a lesser degree than the aMTL subsystem [95]. Maps of cortical atrophy in relation to AD neuropathology generally demonstrate that more prominent neurofibrillary pathology corresponds to greater atrophy in the set of regions encompassed by our overall AD signature of cortical atrophy [96–98]. One recent clinicopathologic study investigated the patterns of atrophy in patients with topographies of pathology subdivided into hippocampal sparing, typical, and limbic predominant [99]. An examination of Fig. 1 [99] reveals that the pattern of atrophy in those with typical pathology corresponds well with our LOAD map, whereas that of the hippocampal sparing group corresponds with our EOAD map. Moreover, the hippocampal sparing group had a mean age of onset of symptoms of 63, whereas the typical pathology group had a mean age of symptom onset of 73. A similar finding has recently been reported using in vivo tau PET imaging [100]. Thus, a small amount of extant data suggests that younger people with AD pathology exhibit strong correspondence between tau pathology and atrophy in a distributed set of brain regions largely concordant with the caudal hippocampal-parahippocampal-retrosplenial subsystem.

3.4. Dissociation of memory performance in EOAD and LOAD

As we reported previously in patients with mild AD dementia [34], impaired performance on the first encoding trial of the AVLT is associated with atrophy in a broad set of left-lateralized isocortical regions, which have been implicated in auditory-verbal working memory and phonologic as well as semantic aspects of language. Auditory-verbal working memory is likely critical to the initial trials of a list-learning memory task and crucial for the transfer of information into long-term storage. Several of the regions found to correlate with the initial trial of the AVLT in the parietal lobe, including the supramarginal and angular gyrus, have been variably associated with the storage function of the phonological loop supporting working memory [101,102]. Some of these regions are involved in both EOAD and LOAD, although we found a more prominent abnormality of verbal encoding in EOAD, consistent with previous observations of working memory impairment in EOAD [103]. In contrast, semantic memory is relatively more impaired in LOAD than EOAD [12,104], which would impact long-term memory encoding. Our previous [105] and current observations of greater anterior temporal atrophy in AD patients who exhibit cued naming impairment and more prominent late-trial auditory-verbal list encoding impairment [34], in conjunction with our present observation of more prominent anterior temporal atrophy and semantic memory impairment in LOAD, provide further behavioral and anatomical support for these ideas. Furthermore, the current finding is consistent with the link between the aMTL, particularly perirhinal cortex, and object-related semantic memory [106]. Taken together, these observations reinforce the importance of both phonologic and semantic language processes in AD, particularly in their contributions to verbal memory. Finally, given the putative role of the rostral hippocampal-perirhinal subsystem for item-level memory, one would predict greater impairment on

recognition memory discrimination in the LOAD group, which was marginally the case, but perhaps made more salient in the context of this group's better overall memory encoding performance.

In addition to providing new insights into the neural systems affected in EOAD versus LOAD, the current findings have practical implications about the nature of tests used in the assessment of patients with EOAD versus LOAD. For example, these data support the notion that measures of immediate memory are sensitive to distributed pathology temporoparietal cortex, reflecting the role of attention and language in list learning. This finding may explain why immediate memory, usually quantified as total learning, has proven to be such a sensitive measure to the early stages of AD, as injury to a number of different neuroanatomical sites might modulate performance [107–110]. Given the early and relatively selective MTL pathology in LOAD, delayed memory tests may provide the most specific measures of early AD in older adults, although challenging measures of semantic memory should also be examined. Most semantic memory measures in standard psychometric batteries suffer from ceiling effects in mildly impaired patients, and tests designed specifically for these populations would be a worthy area of research investigation. At the end of the day, delayed recall measures where impairment may reflect deficits in encoding, storage, or retrieval may be the best tests to apply across the age spectrum of AD because they might enable detection of memory problems at any of these stages but may sacrifice specificity with regard to the underlying pathoanatomical correlates.

3.5. AD as a single versus multiple network disease

In aggregate, groups of mild AD dementia patients demonstrate regional atrophy in a pattern consistent with the predominant involvement of the DMN and portions of the executive control network and dorsal attention network. Yet fractionation of networks and heterogeneity of the disease highlight the oversimplified nature of the AD-DMN model. Our major findings here point out that, even when the overall pattern of AD-related atrophy is superimposed on a crude seven-network parcellation of the cortex, it is clear that the DMN is affected as well as the anterior temporal/paralimbic network—critically important for both episodic and semantic memory function [70]. When a more fine-grained, 17-network model is used, it is clear that AD-related atrophy affects most of the key nodes of the DMN—with the critical exception of most of the medial prefrontal cortex. But it also affects the dorsal language network, which fractionates from the DMN in this more fine-grained model—a fundamentally important point to which other investigators have alluded [70,111,112]. In addition, patients with mild AD dementia show atrophy in the executive control network, dorsal attention network, and visual association network. Furthermore, the heterogeneity of AD dissociates these effects further, with age-related heterogeneity being one major driver of differential network effects. We have demonstrated in multiple prior publications that *APOE* ε4 is another major factor that drives differential network effects [29,33].

Ultimately, if AD originates and progresses through connections of distributed neural networks in the brain [21,113–115], the organization of brain networks will shed light on the topographical differences between typical and atypical AD pathology [116]. We demonstrate here that typical AD dementia patients exhibit atrophy in key nodes of the DMN, anterior temporal network, and language network. However, it is still unclear why and how a critical node of one brain network rather than another becomes selectively vulnerable to AD pathology in the first place [117]. Further investigation is necessary to identify other genetic or possibly environmental drivers of phenotypic diversity in AD and the mechanisms by which age and *APOE* influence the biology and clinical expression of AD. It is also important to acknowledge that increasing age also makes mixed pathologies more common, such as AD with cerebrovascular disease or AD with cortical Lewy body disease; mixed cases present an additional layer of heterogeneity.

Acknowledgments

Data collection and sharing for this project was funded by the Alzheimer's Disease Neuroimaging Initiative (ADNI) (National Institutes of Health grant U01 AG024904) and DOD ADNI (Department of Defense award number W81XWH-12-2-0012). ADNI is funded by the National Institute on Aging, the National Institute of Biomedical Imaging and Bioengineering, and through generous contributions from the following: AbbVie, Alzheimer's Association; Alzheimer's Drug Discovery Foundation; Araclon Biotech; BioClinica, Inc.; Biogen; Bristol-Myers Squibb Company; CereSpir, Inc.; Cogstate; Eisai Inc.; Elan Pharmaceuticals, Inc.; Eli Lilly and Company; Euroimmun; F. Hoffmann-La Roche Ltd. and its affiliated company Genentech, Inc.; Fujirebio; GE Healthcare; IXICO Ltd.; Janssen Alzheimer Immunotherapy Research & Development, LLC.; Johnson & Johnson Pharmaceutical Research & Development LLC.; Lumosity; Lundbeck; Merck & Co., Inc.; Meso Scale Diagnostics, LLC.; NeuroRx Research; Neurotrack Technologies; Novartis Pharmaceuticals Corporation; Pfizer Inc.; Piramal Imaging; Servier; Takeda Pharmaceutical Company; and Transition Therapeutics. The Canadian Institutes of Health Research is providing funds to support ADNI clinical sites in Canada. Private sector contributions are facilitated by the Foundation for the National Institutes of Health (www.fnih.org). The grantee organization is the Northern California Institute for Research and Education, and the study is coordinated by the Alzheimer's Therapeutic Research Institute at the University of Southern California. ADNI data are disseminated by the Laboratory for Neuro Imaging at the University of Southern California.

The authors would also like to acknowledge the following grant support: National Institute of Deafness and Other Communication Disorders (R01 DC014296), National Institute on Aging (R21 AG051987 and R01 AG010124).

RESEARCH IN CONTEXT

1. Systematic review: The authors reviewed the literature using PubMed and AAIC meeting abstracts. Although early-onset Alzheimer's disease has previously been reported as being associated with non-memory cognitive impairment and non-medial temporal lobe cortical atrophy, the relationships between these measures and large-scale brain networks have not previously been investigated. Relevant citations are appropriately cited.
2. Interpretation: In early-onset Alzheimer's disease, cortical neurodegeneration occurs most prominently in different brain networks than in late-onset Alzheimer's disease. These degenerative changes influence clinical presentation in terms of particular characteristics of memory impairment, with early-onset AD patients have more prominent memory encoding impairments and late-onset AD patients having more prominent semantic memory impairment.
3. Future directions: In the future, more specific cognitive tests would illuminate the psychometric characteristics of EOAD versus LOAD in greater detail. Additional investigation is warranted to define additional factors that influence the selective vulnerability of these particular brain regions and networks to AD pathology as a function of age.

References

[1] McKhann G, Drachman D, Folstein M, Katzman R, Price D, Stadlan EM. Clinical diagnosis of Alzheimer's disease: report of the NINCDS-ADRDA Work Group under the auspices of Department of Health and Human Services Task Force on Alzheimer's Disease. Neurology 1984;34:939–44.
[2] McKhann GM, Knopman DS, Chertkow H, Hyman BT, Jack CR Jr, Kawas CH, et al. The diagnosis of dementia due to Alzheimer's disease: Recommendations from the National Institute on Aging and the Alzheimer's Association workgroup. Alzheimers Dement 2011;7:263–9.
[3] Becker JT, Huff FJ, Nebes RD, Holland A, Boller F. Neuropsychological function in Alzheimer's disease. Pattern of impairment and rates of progression. Arch Neurol 1988;45:263–8.
[4] Martin A, Brouwers P, Lalonde F, Cox C, Teleska P, Fedio P, et al. Towards a behavioral typology of Alzheimer's patients. J Clin Exp Neuropsychol 1986;8:594–610.
[5] Barnes J, Dickerson BC, Frost C, Jiskoot LC, Wolk D, van der Flier WM. Alzheimer's disease first symptoms are age dependent: evidence from the NACC dataset. Alzheimers Dement 2015;11:1349–57.
[6] Hof PR, Bouras C, Constantinidis J, Morrison JH. Balint's syndrome in Alzheimer's disease: specific disruption of the occipito-parietal visual pathway. Brain Res 1989;493:368–75.
[7] Johnson JK, Head E, Kim R, Starr A, Cotman CW. Clinical and pathological evidence for a frontal variant of Alzheimer disease. Arch Neurol 1999;56:1233–9.
[8] Kanne SM, Balota DA, Storandt M, McKeel DW Jr, Morris JC. Relating anatomy to function in Alzheimer's disease: neuropsychological profiles predict regional neuropathology 5 years later. Neurology 1998;50:979–85.
[9] Murray ME, Graff-Radford NR, Ross OA, Petersen RC, Duara R, Dickson DW. Neuropathologically defined subtypes of Alzheimer's disease with distinct clinical characteristics: a retrospective study. Lancet Neurol 2011;10:785–96.
[10] Frisoni GB, Testa C, Sabattoli F, Beltramello A, Soininen H, Laakso MP. Structural correlates of early and late onset Alzheimer's disease: voxel based morphometric study. J Neurol Neurosurg Psychiatry 2005;76:112–4.
[11] Frisoni GB, Pievani M, Testa C, Sabattoli F, Bresciani L, Bonetti M, et al. The topography of grey matter involvement in early and late onset Alzheimer's disease. Brain 2007;130:720–30.
[12] Joubert S, Gour N, Guedj E, Didic M, Gueriot C, Koric L, et al. Early-onset and late-onset Alzheimer's disease are associated with distinct patterns of memory impairment. Cortex 2016;74:217–32.
[13] Karas G, Scheltens P, Rombouts S, van Schijndel R, Klein M, Jones B, et al. Precuneus atrophy in early-onset Alzheimer's disease: a morphometric structural MRI study. Neuroradiology 2007;49:967–76.
[14] Moller C, Vrenken H, Jiskoot L, Versteeg A, Barkhof F, Scheltens P, et al. Different patterns of gray matter atrophy in early- and late-onset Alzheimer's disease. Neurobiol Aging 2013;34:2014–22.
[15] Lehmann M, Madison CM, Ghosh PM, Seeley WW, Mormino E, Greicius MD, et al. Intrinsic connectivity networks in healthy subjects explain clinical variability in Alzheimer's disease. Proc Natl Acad Sci U S A 2013;110:11606–11.
[16] Vincent JL, Patel GH, Fox MD, Snyder AZ, Baker JT, Van Essen DC, et al. Intrinsic functional architecture in the anaesthetized monkey brain. Nature 2007;447:83–6.
[17] Smith SM, Fox PT, Miller KL, Glahn DC, Fox PM, Mackay CE, et al. Correspondence of the brain's functional architecture during activation and rest. Proc Natl Acad Sci U S A 2009;106:13040–5.
[18] Buckner RL, Snyder AZ, Shannon BJ, LaRossa G, Sachs R, Fotenos AF, et al. Molecular, structural, and functional characterization of Alzheimer's disease: evidence for a relationship between default activity, amyloid, and memory. J Neurosci 2005;25:7709–17.
[19] Damoiseaux JS, Beckmann CF, Arigita EJ, Barkhof F, Scheltens P, Stam CJ, et al. Reduced resting-state brain activity in the "default network" in normal aging. Cereb Cortex 2008;18:1856–64.
[20] Greicius MD, Srivastava G, Reiss AL, Menon V. Default-mode network activity distinguishes Alzheimer's disease from healthy aging: evidence from functional MRI. Proc Natl Acad Sci U S A 2004;101:4637–42.
[21] Seeley WW, Crawford RK, Zhou J, Miller BL, Greicius MD. Neurodegenerative diseases target large-scale human brain networks. Neuron 2009;62:42–52.
[22] Sperling RA, Laviolette PS, O'Keefe K, O'Brien J, Rentz DM, Pihlajamaki M, et al. Amyloid deposition is associated with impaired default network function in older persons without dementia. Neuron 2009;63:178–88.
[23] Wang L, Zang Y, He Y, Liang M, Zhang X, Tian L, et al. Changes in hippocampal connectivity in the early stages of Alzheimer's disease: evidence from resting state fMRI. Neuroimage 2006;31:496–504.
[24] Buckner RL, Andrews-Hanna JR, Schacter DL. The brain's default network: anatomy, function, and relevance to disease. Ann N Y Acad Sci 2008;1124:1–38.

[25] Albert MS, DeKosky ST, Dickson D, Dubois B, Feldman HH, Fox NC, et al. The diagnosis of mild cognitive impairment due to Alzheimer's disease: recommendations from the National Institute on Aging-Alzheimer's Association workgroups on diagnostic guidelines for Alzheimer's disease. Alzheimers Dement 2011;7:270–9.
[26] Shaw LM, Vanderstichele H, Knapik-Czajka M, Clark CM, Aisen PS, Petersen RC, et al., Alzheimer's Disease Neuroimaging Initiative. Cerebrospinal fluid biomarker signature in Alzheimer's disease neuroimaging initiative subjects. Ann Neurol 2009;65:403–13.
[27] Jack CR Jr, Bernstein MA, Fox NC, Thompson P, Alexander G, Harvey D, et al. The Alzheimer's Disease Neuroimaging Initiative (ADNI): MRI methods. J Magn Reson Imaging 2008;27:685–91.
[28] Bakkour A, Morris JC, Wolk DA, Dickerson BC. The effects of aging and Alzheimer's disease on cerebral cortical anatomy: specificity and differential relationships with cognition. Neuroimage 2013; 76:332–44.
[29] Dickerson BC, Wolk DA, Alzheimer's Disease Neuroimaging Initiative. Dysexecutive versus amnesic phenotypes of very mild Alzheimer's disease are associated with distinct clinical, genetic and cortical thinning characteristics. J Neurol Neurosurg Psychiatry 2011;82:45–51.
[30] Dickerson BC, Wolk DA, On behalf of the Alzheimer's Disease Neuroimaging Initiative. MRI cortical thickness biomarker predicts AD-like CSF and cognitive decline in normal adults. Neurology 2012; 78:84–90.
[31] Dickerson BC, Wolk DA, Alzheimer's Disease Neuroimaging Initiative. Biomarker-based prediction of progression in MCI: comparison of AD signature and hippocampal volume with spinal fluid amyloid-beta and tau. Front Aging Neurosci 2013;5:55.
[32] Dickerson BC, Fenstermacher E, Salat DH, Wolk DA, Maguire RP, Desikan R, et al. Detection of cortical thickness correlates of cognitive performance: Reliability across MRI scan sessions, scanners, and field strengths. Neuroimage 2008;39:10–8.
[33] Wolk DA, Dickerson BC, Alzheimer's Disease Neuroimaging Initiative. Apolipoprotein E (APOE) genotype has dissociable effects on memory and attentional-executive network function in Alzheimer's disease. Proc Natl Acad Sci U S A 2010;107:10256–61.
[34] Wolk DA, Dickerson BC, Alzheimer's Disease Neuroimaging Initiative. Fractionating verbal episodic memory in Alzheimer's disease. Neuroimage 2011;54:1530–9.
[35] Rey A. L'examen clinique en psychologie Paris. Paris: Presses Universitaires de France; 1964.
[36] Snodgrass JG, Corwin J. Pragmatics of measuring recognition memory: applications to dementia and amnesia. J Exp Psychol Gen 1988; 117:34–50.
[37] Kaplan E, Goodglass H, Weintraub S. The Boston Naming Test. Philadelphia: Lea and Febiger; 1983.
[38] Augustinack JC, Huber KE, Stevens AA, Roy M, Frosch MP, van der Kouwe AJ, et al., Alzheimer's Disease Neuroimaging Initiative. Predicting the location of human perirhinal cortex, Brodmann's area 35, from MRI. Neuroimage 2013;64:32–42.
[39] Fischl B, Stevens AA, Rajendran N, Yeo BT, Greve DN, Van Leemput K, et al. Predicting the location of entorhinal cortex from MRI. Neuroimage 2009;47:8–17.
[40] Dickerson BC, Bakkour A, Salat DH, Feczko E, Pacheco J, Greve DN, et al. The cortical signature of Alzheimer's disease: regionally specific cortical thinning relates to symptom severity in very mild to mild AD dementia and is detectable in asymptomatic amyloid-positive individuals. Cereb Cortex 2009;19:497–510.
[41] Canu E, Frisoni GB, Agosta F, Pievani M, Bonetti M, Filippi M. Early and late onset Alzheimer's disease patients have distinct patterns of white matter damage. Neurobiol Aging 2012;33:1023–33.
[42] Cavedo E, Pievani M, Boccardi M, Galluzzi S, Bocchetta M, Bonetti M, et al. Medial temporal atrophy in early and late-onset Alzheimer's disease. Neurobiol Aging 2014;35:2004–12.
[43] Ishii K, Kawachi T, Sasaki H, Kono AK, Fukuda T, Kojima Y, et al. Voxel-based morphometric comparison between early- and late-onset mild Alzheimer's disease and assessment of diagnostic performance of z score images. AJNR Am J Neuroradiol 2005;26:333–40.
[44] McDonald WM, Krishnan KR, Doraiswamy PM, Figiel GS, Husain MM, Boyko OB, et al. Magnetic resonance findings in patients with early-onset Alzheimer's disease. Biol Psychiatry 1991;29:799–810.
[45] Shiino A, Watanabe T, Maeda K, Kotani E, Akiguchi I, Matsuda M. Four subgroups of Alzheimer's disease based on patterns of atrophy using VBM and a unique pattern for early onset disease. Neuroimage 2006;33:17–26.
[46] Shiino A, Watanabe T, Kitagawa T, Kotani E, Takahashi J, Morikawa S, et al. Different atrophic patterns in early- and late-onset Alzheimer's disease and evaluation of clinical utility of a method of regional z-score analysis using voxel-based morphometry. Dement Geriatr Cogn Disord 2008;26:175–86.
[47] van de Pol LA, Hensel A, Barkhof F, Gertz HJ, Scheltens P, van der Flier WM. Hippocampal atrophy in Alzheimer disease: age matters. Neurology 2006;66:236–8.
[48] Woo JI, Kim JH, Lee JH. Age of onset and brain atrophy in Alzheimer's disease. Int Psychogeriatr 1997;9:183–96.
[49] Andrews-Hanna JR, Reidler JS, Sepulcre J, Poulin R, Buckner RL. Functional-anatomic fractionation of the brain's default network. Neuron 2010;65:550–62.
[50] Dickerson BC, Eichenbaum H. The episodic memory system: neurocircuitry and disorders. Neuropsychopharmacology 2010;35:86–104.
[51] Wolk DA, Budson AE. Memory systems. Continuum (Minneap Minn) 2010;16:15–28.
[52] Uncapher MR, Otten LJ, Rugg MD. Episodic encoding is more than the sum of its parts: an fMRI investigation of multifeatural contextual encoding. Neuron 2006;52:547–56.
[53] Buckner RL, Wheeler ME. The cognitive neuroscience of remembering. Nat Rev Neurosci 2001;2:624–34.
[54] Dobbins IG, Foley H, Schacter DL, Wagner AD. Executive control during episodic retrieval: multiple prefrontal processes subserve source memory. Neuron 2002;35:989–96.
[55] Farovik A, Dupont LM, Arce M, Eichenbaum H. Medial prefrontal cortex supports recollection, but not familiarity, in the rat. J Neurosci 2008;28:13428–34.
[56] Burwell RD, Amaral DG. Cortical afferents of the perirhinal, postrhinal, and entorhinal cortices of the rat. J Comp Neurol 1998; 398:179–205.
[57] Suzuki WA, Amaral DG. Perirhinal and parahippocampal cortices of the macaque monkey: cortical afferents. J Comp Neurol 1994; 350:497–533.
[58] Witter MP, Wouterlood FG, Naber PA, Van Haeften T. Anatomical organization of the parahippocampal-hippocampal network. Ann N Y Acad Sci 2000;911:1–24.
[59] Aggleton JP, Wright NF, Vann SD, Saunders RC. Medial temporal lobe projections to the retrosplenial cortex of the macaque monkey. Hippocampus 2012;22:1883–900.
[60] Strange BA, Witter MP, Lein ES, Moser EI. Functional organization of the hippocampal longitudinal axis. Nat Rev Neurosci 2014; 15:655–69.
[61] Kahn I, Andrews-Hanna JR, Vincent JL, Snyder AZ, Buckner RL. Distinct cortical anatomy linked to subregions of the medial temporal lobe revealed by intrinsic functional connectivity. J Neurophysiol 2008;100:129–39.
[62] Ranganath C, Ritchey M. Two cortical systems for memory-guided behaviour. Nat Rev Neurosci 2012;13:713–26.
[63] Hoistad M, Barbas H. Sequence of information processing for emotions through pathways linking temporal and insular cortices with the amygdala. Neuroimage 2008;40:1016–33.
[64] Insausti R, Amaral DG. Entorhinal cortex of the monkey: IV. Topographical and laminar organization of cortical afferents. J Comp Neurol 2008;509:608–41.
[65] Munoz M, Insausti R. Cortical efferents of the entorhinal cortex and the adjacent parahippocampal region in the monkey (Macaca fascicularis). Eur J Neurosci 2005;22:1368–88.

[66] Price JL. Definition of the orbital cortex in relation to specific connections with limbic and visceral structures and other cortical regions. Ann N Y Acad Sci 2007;1121:54–71.
[67] Jackson RL, Hoffman P, Pobric G, Lambon Ralph MA. The nature and neural correlates of semantic association versus conceptual similarity. Cereb Cortex 2015;25:4319–33.
[68] Patterson K, Nestor PJ, Rogers TT. Where do you know what you know? The representation of semantic knowledge in the human brain. Nat Rev Neurosci 2007;8:976–87.
[69] Man K, Kaplan J, Damasio H, Damasio A. Neural convergence and divergence in the mammalian cerebral cortex: from experimental neuroanatomy to functional neuroimaging. J Comp Neurol 2013; 521:4097–111.
[70] Pascual B, Masdeu JC, Hollenbeck M, Makris N, Insausti R, Ding SL, et al. Large-scale brain networks of the human left temporal pole: a functional connectivity MRI study. Cereb Cortex 2015; 25:680–702.
[71] Kobayashi Y, Amaral DG. Macaque monkey retrosplenial cortex: II. Cortical afferents. J Comp Neurol 2003;466:48–79.
[72] Kobayashi Y, Amaral DG. Macaque monkey retrosplenial cortex: III. Cortical efferents. J Comp Neurol 2007;502:810–33.
[73] Lavenex P, Suzuki WA, Amaral DG. Perirhinal and parahippocampal cortices of the macaque monkey: projections to the neocortex. J Comp Neurol 2002;447:394–420.
[74] Arnold SE, Hyman BT, Flory J, Damasio AR, Van Hoesen GW. The topographical and neuroanatomical distribution of neurofibrillary tangles and neuritic plaques in the cerebral cortex of patients with Alzheimer's disease. Cereb Cortex 1991;1:103–16.
[75] Braak H, Braak E. Neuropathological stageing of Alzheimer-related changes. Acta Neuropathol 1991;82:239–59.
[76] Jack CR Jr, Knopman DS, Jagust WJ, Shaw LM, Aisen PS, Weiner MW, et al. Hypothetical model of dynamic biomarkers of the Alzheimer's pathological cascade. Lancet Neurol 2010;9:119–28.
[77] Wolk DA, Das SR, Mueller SG, Weiner MW, Yushkevich PA, Alzheimer's Disease Neuroimaging Initiative. Medial temporal lobe subregional morphometry using high resolution MRI in Alzheimer's disease. Neurobiol Aging 2017;49:204–13.
[78] Frisoni GB, Prestia A, Rasser PE, Bonetti M, Thompson PM. In vivo mapping of incremental cortical atrophy from incipient to overt Alzheimer's disease. J Neurol 2009;256:916–24.
[79] Mahley RW, Weisgraber KH, Huang Y. Apolipoprotein E4: a causative factor and therapeutic target in neuropathology, including Alzheimer's disease. Proc Natl Acad Sci U S A 2006;103:5644–51.
[80] Brecht WJ, Harris FM, Chang S, Tesseur I, Yu GQ, Xu Q, et al. Neuron-specific apolipoprotein e4 proteolysis is associated with increased tau phosphorylation in brains of transgenic mice. J Neurosci 2004;24:2527–34.
[81] Crary JF, Trojanowski JQ, Schneider JA, Abisambra JF, Abner EL, Alafuzoff I, et al. Primary age-related tauopathy (PART): a common pathology associated with human aging. Acta Neuropathol 2014; 128:755–66.
[82] Vincent JL, Kahn I, Van Essen DC, Buckner RL. Functional connectivity of the macaque posterior parahippocampal cortex. J Neurophysiol 2010;103:793–800.
[83] Parvizi J, Van Hoesen GW, Buckwalter J, Damasio A. Neural connections of the posteromedial cortex in the macaque. Proc Natl Acad Sci U S A 2006;103:1563–8.
[84] Margulies DS, Vincent JL, Kelly C, Lohmann G, Uddin LQ, Biswal BB, et al. Precuneus shares intrinsic functional architecture in humans and monkeys. Proc Natl Acad Sci U S A 2009; 106:20069–74.
[85] Barbas H, Ghashghaei H, Dombrowski SM, Rempel-Clower NL. Medial prefrontal cortices are unified by common connections with superior temporal cortices and distinguished by input from memory-related areas in the rhesus monkey. J Comp Neurol 1999; 410:343–67.
[86] Vincent JL, Snyder AZ, Fox MD, Shannon BJ, Andrews JR, Raichle ME, et al. Coherent spontaneous activity identifies a hippocampal-parietal memory network. J Neurophysiol 2006; 96:3517–31.
[87] Wagner AD, Shannon BJ, Kahn I, Buckner RL. Parietal lobe contributions to episodic memory retrieval. Trends Cogn Sci 2005; 9:445–53.
[88] Svoboda E, McKinnon MC, Levine B. The functional neuroanatomy of autobiographical memory: a meta-analysis. Neuropsychologia 2006;44:2189–208.
[89] Buckner RL, Carroll DC. Self-projection and the brain. Trends Cogn Sci 2007;11:49–57.
[90] Hassabis D, Maguire EA. Deconstructing episodic memory with construction. Trends Cogn Sci 2007;11:299–306.
[91] Schacter DL, Addis DR, Buckner RL. Remembering the past to imagine the future: the prospective brain. Nat Rev Neurosci 2007; 8:657–61.
[92] Mullally SL, Maguire EA. A new role for the parahippocampal cortex in representing space. J Neurosci 2011;31:7441–9.
[93] Bar M, Aminoff E, Schacter DL. Scenes unseen: the parahippocampal cortex intrinsically subserves contextual associations, not scenes or places per se. J Neurosci 2008;28:8539–44.
[94] Jenkins LJ, Ranganath C. Prefrontal and medial temporal lobe activity at encoding predicts temporal context memory. J Neurosci 2010; 30:15558–65.
[95] Dickerson BC, Feczko E, Augustinack JC, Pacheco J, Morris JC, Fischl B, et al. Differential effects of aging and Alzheimer's disease on medial temporal lobe cortical thickness and surface area. Neurobiol Aging 2009a;30:432–40.
[96] Kotrotsou A, Schneider JA, Bennett DA, Leurgans SE, Dawe RJ, Boyle PA, et al. Neuropathologic correlates of regional brain volumes in a community cohort of older adults. Neurobiol Aging 2015; 36:2798–805.
[97] Vemuri P, Simon G, Kantarci K, Whitwell JL, Senjem ML, Przybelski SA, et al. Antemortem differential diagnosis of dementia pathology using structural MRI: differential-STAND. Neuroimage 2011;55:522–31.
[98] Whitwell JL, Josephs KA, Murray ME, Kantarci K, Przybelski SA, Weigand SD, et al. MRI correlates of neurofibrillary tangle pathology at autopsy: a voxel-based morphometry study. Neurology 2008; 71:743–9.
[99] Whitwell JL, Dickson DW, Murray ME, Weigand SD, Tosakulwong N, Senjem ML, et al. Neuroimaging correlates of pathologically defined subtypes of Alzheimer's disease: a case-control study. Lancet Neurol 2012;11:868–77.
[100] Schwarz AJ, Yu P, Miller BB, Shcherbinin S, Dickson J, Navitsky M, et al. Regional profiles of the candidate tau PET ligand 18F-AV-1451 recapitulate key features of Braak histopathological stages. Brain 2016;139:1539–50.
[101] Buchsbaum BR, D'Esposito M. The search for the phonological store: from loop to convolution. J Cogn Neurosci 2008; 20:762–78.
[102] Buchsbaum BR, Baldo J, Okada K, Berman KF, Dronkers N, D'Esposito M, et al. Conduction aphasia, sensory-motor integration, and phonological short-term memory—an aggregate analysis of lesion and fMRI data. Brain Lang 2011;119:119–28.
[103] Stopford CL, Thompson JC, Neary D, Richardson AM, Snowden JS. Working memory, attention, and executive function in Alzheimer's disease and frontotemporal dementia. Cortex 2012;48:429–46.
[104] Grosse DA, Gilley DW, Wilson RS. Episodic and semantic memory in early versus late onset Alzheimer's disease. Brain Lang 1991; 41:531–7.
[105] Domoto-Reilly K, Sapolsky D, Brickhouse M, Dickerson BC, Alzheimer's Disease Neuroimaging Initiative. Naming impairment in Alzheimer's disease is associated with left anterior temporal lobe atrophy. Neuroimage 2013;63:348–55.

[106] Clarke A, Tyler LK. Understanding what we see: how we derive meaning from vision. Trends Cogn Sci 2015;19:677–87.
[107] Albert MS, Moss MB, Tanzi R, Jones K. Preclinical prediction of AD using neuropsychological tests. J Int Neuropsychol Soc 2001; 7:631–9.
[108] Blacker D, Lee H, Muzikansky A, Martin EC, Tanzi R, McArdle JJ, et al. Neuropsychological measures in normal individuals that predict subsequent cognitive decline. Arch Neurol 2007; 64:862–71.
[109] Petersen RC, Smith GE, Ivnik RJ, Kokmen E, Tangalos EG. Memory function in very early Alzheimer's disease. Neurology 1994;44:867–72.
[110] Tierney MC, Yao C, Kiss A, McDowell I. Neuropsychological tests accurately predict incident Alzheimer disease after 5 and 10 years. Neurology 2005;64:1853–9.
[111] Binder JR, Desai RH, Graves WW, Conant LL. Where is the semantic system? A critical review and meta-analysis of 120 functional neuroimaging studies. Cereb Cortex 2009;19:2767–96.
[112] Jackson RL, Hoffman P, Pobric G, Lambon Ralph MA. The semantic network at work and rest: differential connectivity of anterior temporal lobe subregions. J Neurosci 2016;36:1490–501.
[113] Mesulam MM. Neuroplasticity failure in Alzheimer's disease: bridging the gap between plaques and tangles. Neuron 1999; 24:521–9.
[114] Sanders DW, Kaufman SK, DeVos SL, Sharma AM, Mirbaha H, Li A, et al. Distinct tau prion strains propagate in cells and mice and define different tauopathies. Neuron 2014;82:1271–88.
[115] Zhou J, Gennatas ED, Kramer JH, Miller BL, Seeley WW. Predicting regional neurodegeneration from the healthy brain functional connectome. Neuron 2012;73:1216–27.
[116] Warren JD, Fletcher PD, Golden HL. The paradox of syndromic diversity in Alzheimer disease. Nat Rev Neurol 2012;8:451–64.
[117] Hof PR, Morrison JH. Hippocampal and neocortical involvement in normal brain aging and dementia: morphological and neurochemical profile of the vulnerable circuits. J Am Geriatr Soc 1996;44:857–64.